University of HUDDERSFIELD
University of Huddersfield Press

Fields: journal of Huddersfield student research
Available open access at: https://www.fieldsjournal.org.uk/

FIELDS Journal of Huddersfield student research

Investigating the performance of rail steels

Daniel Herbert Woodhead

University of Huddersfield, Queensgate, Huddersfield, West Yorkshire, HD1 3DH

ARTICLE INFO

Article history:
Received 18 October 2020
Received in revised form 15 February 2021
Accepted 27 April 2021

Keywords:
Rolling contact fatigue
Wear
Rail damage mechanisms
Tensile test
Twin disc test
Whole life rail model
Material properties
Percentage elongation
Hardness
Yield strength
Young's modulus
Ultimate tensile strength

ABSTRACT

This study focusses on aiding the understanding of how various material properties affect rolling the contact fatigue (RCF) and wear of rail steels. This will support the future development of RCF prediction models, and in the identification of rail damage mechanisms. Tensile tests were conducted on several rail steel samples and compared to wear, and RCF data available in literature (Burstow, 2009), to try and meet the aim of this research. The findings from this study support the statements that hardness is a good indicator of ultimate tensile strength and that steel samples from the head and foot of rails have quite different yield strengths (max 24% difference). The strongest outcome of this research is data supporting claims that a ratio of the product of young's modulus squared and percentage elongation to hardness cubed ($(E^2*P_e)/H^3$) had a much better correlation (R^2=0.98) to wear data than just hardness (R^2=0.89). As well as this, new ideas for characterizing Mark Burstow's whole life rail model have been presented in this study, due to the importance of understanding how material properties impact rolling contact fatigue and wear. It is suggested in this study that the Tγ Threshold and Tγ Balance of a material could be calculated using ultimate tensile strength (UTS) and not hardness, due to findings showing a higher correlation between the number of cycles to RCF initiation and UTS (R^2 = 1.0), than with hardness (R^2 = 0.975).

Nomenclature

Symbol	Definition	Unit
A	Contact Patch Area	m^2
E	Young's Modulus	Pa
H	Hardness	HB
k	Adhesive Wear Coefficient.	-
Lf	Final Length	m
Lo	Original Length	m
N	Normal Contact Force	N
Pe	Percentage Elongation	%
R1 and R2	Radius of each body	m
R^2	Correlation Coefficient	-
ro	Mean Rolling Radius	m
s	Slip Distance	m
Tγ	Creepage Force (T-Gamma)	Nm
V	Velocity	m/s
v	Volume of lost material	m^3
α	Yaw Angle	rad/s
γx	Longitudinal Creep	m or %
γy	Lateral Creep	m or %
ζ	Algebraic Value which is Different for each Wheel	-
μ	Coefficient of Friction	-
σ	Stress	Pa
ξ	Strain	-

INTRODUCTION

Problem statement

Railway wheels and rails are highly susceptible to damage due to the large forces acting through the minute contact patch where they interact, over a high number of cycles of operation. These contact patches can be as small as ~13mm in diameter (Hernandez, 2008), meaning that understanding these forces is a fundamental piece of information that any rail engineer should consider when ensuring the safe and economical operation of a railway (Shebani & Iwnicki, 2016). A photograph of Huddersfield railway station can be seen in Figure 1.

As time has progressed there has been an increasing demand on the railway to support trains with higher axle load capabilities, higher velocities and support increased rail traffic. These influential factors mean that the rail industry must ensure that a safe and maintainable track infrastructure is in place, one that is tightly monitored to avoid catastrophic failure due to degradation on the track (Shebani & Iwnicki, 2016).

Figure 1: A photograph of Huddersfield railway station.

Literature review

The foundation of this study contains a concise literature review of research in the field of rail steel testing, as well as the current industry measurement standards.

Twin disc testing

Twin disc testing is commonly used in the rail industry to test the damage function resistance of various rail steels, whilst trying to best simulate the conditions encountered on track. These tests are preferrable due to the high level of control they offer over the test conditions available, as well as the relative simplicity of manufacturing testing specimens at a lower cost than full scale components (Lewis, et al., 2017). A typical twin disc machine utilizes two discs which are driven by independent motors to allow for the slip to be controlled and measured. A loading cell or loading arm is used to load the upper disc against the lower disc and to replicate the scaled normal force experienced at full scale conditions (Galas, Smejkal, Omasta, & Hartl, 2014).

Currently there is much debate by researchers as to how to scale the full-scale conditions encountered on track to twin disc scale. This has led to many different investigations of wear and rolling contact fatigue (RCF) being developed using various twin disc rig configurations, with no standard methodology being agreed upon. This is highly problematic as the results from each of the different tests cannot be compared (Lewis, et al., 2017). Some scholars will use an energy-based approach to scaling, following the British Rail Research or University of Sheffield model, which both use the T-Gamma value developed by British Rail Research. They may alternatively use the KTH model developed by the Royal Institute of Technology, which is a non-energy-based approach that follows Archard's theory (Quost, et al., 2010). These theories will be expanded upon in later sections of this article.

Tensile testing

Tensile testing is used in the rail industry as a means of measuring rail steel's mechanical properties. This is done by stretching a material to destruction and measuring the extension. Tensile testing can be used to find material properties for use in finite element analysis, which is commonly used in the railway to solve many rail problems (Bandula-Heva & Dhanasekar, 2011). Tensile tests are used to create stress-strain graphs for various rail steel materials, as they are required to understand the behavior of the rail head under wheel loading (Bandula-Heva & Dhanasekar, 2011).

Hardness testing

Hardness is a highly considered parameter when selecting a rail steel for use on a section of track. This is highlighted by the fact that most, if not all, rail steels include their hardness value in their name, e.g., R260 grade steel has a Brinell hardness of 260HB. To this end, hardness testing has become an instrumental part of predicting the damage of

rail steels, as highlighted in Archard's theory, which will be discussed in a future section of this article.
Hardness testing is important, as it can give insight into the effects of damage mechanisms on rail steels. For example, in the paper entitled "Investigation of the influence of rail hardness on the wear of rail and wheel materials under dry conditions (ICRI wear mapping project)," wear rate is plotted against a variety of rail steels with varying hardness values. Furthermore, hardness mapping is conducted to view the hardness values at different depths from the surface of different rail specimens, to see if this affects wear. This showed some of the general trends of wear and hardness but gave little explanation as to why this happens. It is highlighted in this paper that a lack of material knowledge could have contributed to this conclusion, amongst other potential issues highlighted (Lewis, et al., 2019).

Current research

Many papers have attempted to use a combination of twin disc testing, tensile testing and hardness testing to develop or verify damage function models for rail steels. A good example of twin disc testing can be seen in a paper written by Martin Hiensch, entitled 'Rolling contact fatigue: damage function development from two-disc test data.' In this paper, on-track observations are used to test R220 grade steel under scaled conditions representative of the full-scale conditions. The findings from the twin disc tests conducted are then compared to Mark Burstow's whole life rail model and seem to help verify it, thus showing the importance of rail steel testing in verifying damage function models (Hiensch & Burgelman, 2018).

Tensile testing has recently been used by Mark Burstow to attempt to characterize his whole life rail model using material properties (Burstow, 2009). The necessity for linking material properties with damage mechanisms is highlighted by the lack of inclusion of material properties in all major damage function models. Archard's theory includes only hardness in its calculation and $T\gamma$ model includes no material properties. To the authors knowledge only Burstow has attempted to make the link between damage mechanisms and other material properties (Burstow, 2009). This is a good step into the right direction with regards to improving the link between material properties and damage mechanisms, as it has long been thought that hardness has the biggest impact on damage mechanisms, which is shown in models such as Archard's wear model.

Improving the understanding of the links between material/mechanical properties to damage functions should help to improve the understanding of rail steel performance. The current understanding in the rail industry is that higher hardness results in better wear resistance properties, however in some cases such as HP335 grade steel, the grade performs much better than steels of similar hardness (British Steel, 2020). This was shown in tests conducted by Network rail who recorded damage function data at different track sites for comparison to standard grade steels (SUSTRAIL, n.d.). This anomaly shows a necessity for further understanding which other material properties may attribute to increased wear and RCF resistance, which is what this paper will attempt to do.

Measurement Standards

Rail steels must be rigorously tested before use on track which is the reason why standards such as the EN13674-1 2017 exist. This standard contains only nine pearlitic steels with varying hardness values (Bevan, Jaiswal, Smith , & Cabral, 2018). BS11 was the very first British standard issued to rail steel manufacturers that specified a minimum tensile strength requirement of 618 N mm-^{2}. In 1985 this was revised to 710 N mm-^{2} for standard grade steels and to 880 N mm-^{2} for wear resistive grades (Yates, 1996). It is curious that these material properties are mentioned in the standards but are not yet included in any wear or RCF models to the authors knowledge. They are important parameters that are highlighted by the standards, and hence may have some impact on the damage function resistance of a rail steel. These standards also help to show why tensile testing has become an instrumental part of rail steel testing.

Research aim

This research will attempt to offer a better understanding of the link between material properties and the damage mechanisms of rails. Improving the understanding of rail steel performance will have a large benefit to the rail industry as it can be applied to their existing infrastructure to help optimise cost savings through maintenance. If the rail industry understands which steels are most resistant to wear and rolling contact fatigue (RCF), and why, then they can then optimise their infrastructure and planned maintenance, as well as save money by planning where to utilize premium steels more effectively.

BACKGROUND RESEARCH

As well as a literature review this study is comprised of concise background knowledge regarding damage mechanisms of railway rails, as well as relevant material properties, to ensure that the reader has the necessary underlying understanding of the parameters and tests included in this study.

Wheel-rail contact

To begin to understand damage mechanisms it is imperative to first grasp the fundamentals of what is happening at the wheel-rail interface and the various forces, which act over many cycles of operation. These forces can occur at contact patches as small as 20 pence coins and can cause large stresses of approximately 3000 MPa to act between the wheel and rail (Hernandez, 2008). These stresses are responsible for plastic flow, wear, and fatigue damage, which are commonly referred to as damage mechanisms (Molyneux-Berry, Davis, & Bevan, 2014).

Normal contact

Normal contact describes the stresses, pressures and deformations that occur when elastic and spherical bodies interact with each other in frictionless contact (Hertz, 1881/1896). The contact patches between the two contacting bodies tend to be elliptical (Wang & Chung, 2013) and can be found using either finite element analysis (FEA) or Hertzian contact theory. These methods can be used to find the stresses acting at the contact patch between a railway wheel and rail.

Tangential contact

The contact patch between rail and wheel is where the tangential forces will act. These forces include the traction and braking forces, as well as guiding and parasitic forces (Iwnicki, 2006). These parasitic forces do not contribute to the desired motion of the train. Due to the previously discussed elasticity that occurs between a wheel and a rail, caused by the normal contact force, some points at the contact patch may slip while other points may stick when the two bodies move relative to each other. This slip is referred to as creepage and this creepage is responsible for generating tangential creep forces and spin moments (ZaaZaa & Schwab, 2009). Understanding the various creepages is important as it plays a large part in wear at the wheel-rail interface, especially in the Tγ model. These creepages can be found using Kalker's theory, explained below.

If a wheel that is assumed frictionless is freely moving down a track or especially around a curve, then due to the conicity and the different rolling radii of each body (R1 and R2), a longitudinal creep force is created. Longitudinal creepage (γ_x) at the contact patch is also dictated by the angular speed of the wheelset (ω) and linear velocity (V):

$$\gamma_x = \frac{R\omega - V}{V} \quad (1)$$

In quasi- static conditions, the lateral creepage (γ_y) is the yaw angle (α) common between two wheels (Iwnicki, 2006):

$$\gamma_y = -\alpha \quad (2)$$

In quasi-static conditions the rail speed (V) is zero and can be simplified. Spin creepage (γ_s) can be found using the below equation (Iwnicki, 2006):

$$\gamma_s = \sin\zeta / r_o \quad (3)$$

ζ is an algebraic value which is different for each wheel. This expression shows spin creepage is more prevalent when flange contact occurs and is a larger value on smaller radii wheels (Iwnicki, 2006). The various creepages outlined can be seen in Figure 2.

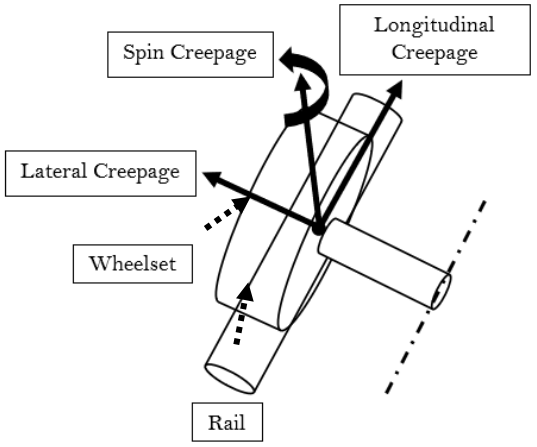

Figure 2: An illustration of the various creepages acting at the wheel-rail contact patch.

Damage mechanisms

There are many mechanisms that can cause damage to railway wheels and tracks, each of which are prevalent under different track conditions. Understanding these mechanisms is critical to help extend the life expectancy of tracks and wheels.

Wear

Wear is defined as the removal of material from a solid surface by mechanical action (Shebani & Iwnicki, 2016). The wear rate of a rail or wheel is a critical parameter to understand for planning maintenance as it can be used to predict the life expectancy of the part in question.

Archard's theory

A current method of predicting wear rate using material properties is Archard's theory, which suggests that the wear volume (v) is proportional to the product of normal contact force (N) and slip distance (s) (Martins, 2001). The slip distance is the creepage expressed in terms of distance. It also suggests that wear volume is inversely proportional to the hardness of a material (H). The equation is as follows, where 'k' is an adhesive wear coefficient:

$$v = \frac{k\,N\,s}{H} \tag{4}$$

T-gamma models

Wear number (Tγ) was originally introduced by British Rail Research (Braghin et al., 2006) in their BRR wear model. Tγ is physically just the energy dissipated from the train's wheels to the rail through the wheel rail interface, when in slip. It can also be thought of as the contact patch frictional energy (Burstow, 2012). The lateral and longitudinal creep forces (T_x and T_y) of the train and the lateral and longitudinal creepages (γ_x and γ_y) can be used to find Tγ:

$$T\gamma = T_x\gamma_x + T_y\gamma_y \tag{5}$$

These Tγ values can then be used in wear functions and compared to wear regimes to find the severity of wear (Network Rail, 2012).

The University of Sheffield has also developed a model that uses Tγ. They propose that Tγ/A, 'A' being the contact patch area, would be a better representation of what happens at the wheel rail interface (Pombo, Ambrosio, Pereira, & others, 2010). The University of Sheffield model concludes the same as the BRR model, that wear is more dominant at higher Tγ values. It is important to note that neither wear model includes any material properties in its determination of wear.

RCF prediction modelling

Rolling-contact fatigue (RCF) is defined as a failure or material removal driven by crack propagation caused by the near-surface alternating stress field (Akchurin, 2017). It is important to understand the conditions that can cause RCF and various models have attempted to do this.

Whole life rail model

Investigating RCF damage to rails or wheels can be done using the whole life rail model, developed by Mark Burstow (Burstow, 2009). According to the model, fatigue damage is dependent on the frictional energy at the rail contact patch (Tγ). This can be best seen in Figure 3, which shows a whole life rail model damage function graph. This model can be used to show the conditions that create both wear and RCF. Whilst developed, and strictly only valid, for R260 grade steel, this graph has been further characterized by Burstow using various material properties.

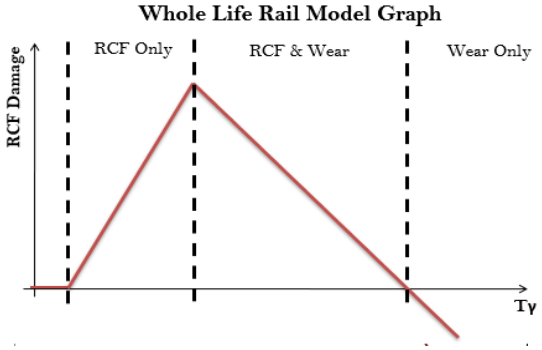

Figure 3: An example of a whole life rail model graph (Burstow, 2009).

Shakedown theory

Shakedown theory attempts to directly show the links between material properties and RCF. It does this by correlating critical shear stress, normal contact stress and the tractional coefficient at the contact patch. It is expected from this method that RCF will occur above the shakedown limit (Muhamedsalih, Stow, & Bevan, 2018). This method however does not account for increasing wear rate, which reduces and removes the RCF crack propagation.

Material properties

It is important to understand material properties and how they may link to the damage mechanisms. This is the basis of choosing the correct materials for use on rails and railway wheels.

Material microstructure

To understand the material properties of typical rail steels, it is important to see the material microstructure. The microstructure of rail steels commonly will consist fully of pearlite or pearlitic steel, as seen in Figure 4. Pearlite is formed during a slow cooling process that is characterized by the joint arrangement of thin layers of ferrite and cementite (D.Raabe, N/A). It is these thin layers of cementite and small inter-lamellar spacings that give rail steels such high wear resistive properties compared to other steels.

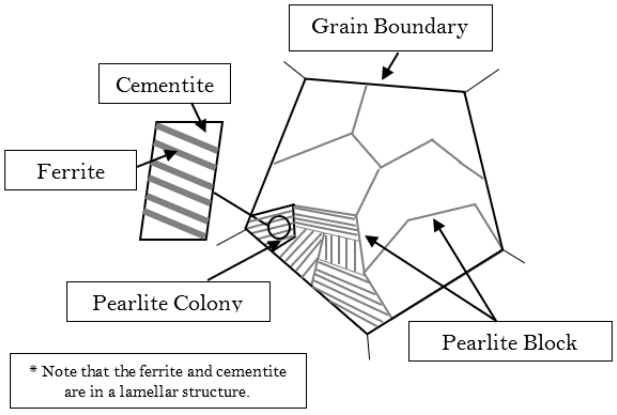

Figure 4: An illustration heavily inspired by (Tomoya, Shigeru, & Hamanda , 2013), on the microstructure of a typical rail steel.

Hardness

Hardness is defined as a materials ability to resist plastic deformation (Peter, 2007). It is very typical of rail steels to include a value of Brinell hardness in their name, for example R200 and R260b steel. This shows that hardness is highly considered when selecting a material for rails and wheels. This fits in with Archard's theory as harder materials would implicitly have a better wear resistance. Pearlitic rail steels also become much harder under work hardening conditions which is why they are favored for their wear resistive properties.

Ultimate tensile strength

Ultimate tensile strength (UTS) is defined as the maximum stress a material can undergo when in compression or tension. It is the highest stress a material can undergo and its maximum resistance to fracture (CORROSIONPEDIA, 2018).

Young's modulus

Youngs modulus (E) describes the elastic properties of a solid under tension and compression in one direction. It is a measure of a materials ability to withstand changes in length caused by tension and compression (Britannica, N/A). Mathematically it is the longitudinal stress (σ) divided by the strain (ξ):

$$E = \frac{\sigma}{\xi} \quad (6)$$

Many authors believe that the fracture strain of a material is related to wear of a solid body. The fracture strain being dependent on the ratio of hardness (H) to young's modulus (E). The higher this ratio and with a moderately high hardness, the better wear resistance a material is said to have (Wangyang, Cheng, Lukitsch, Weiner, & Lev, 2004).

Yield strength

Yield strength is the point at which a material enters the plastic deformation region. Where the point of yield is not easily defined, a proof stress is sometimes taken instead, this is commonly where 0.2 percent plastic deformation occurs (Wikipedia, 2020).

Percentage elongation

Percentage elongation (P_e) is the amount of plastic and elastic deformation that can occur in a material up to the point of fracture. To calculate this parameter, the original length (L_o) is compared to the final length (L_f), giving the following equation:

$$P_e(\%) = \frac{L_f - L_o}{L_o} \times 100 \quad (7)$$

Percentage elongation is useful for finding the ductility of a material and can be used to give a general sense of malleability and toughness properties (CORROSIONPEDIA, 2018).

TESTING METHODOLOGY

The key to acquiring the mechanical, RCF and wear properties of several steel specimens was to conduct a tensile test and a twin disc test. These parameters

were then going to be compared to each other to show any links between them.

Tensile testing

Tensile tests were conducted at the Institute of Railway Research (IRR) using an Instron 8874 tensile machine, seen in Figure 5, to stretch fourteen rail steel samples, seven from the head of a rail and seven from the foot, to destruction. The young's modulus, ultimate tensile strength, yield strength and percentage elongation of each were calculated.

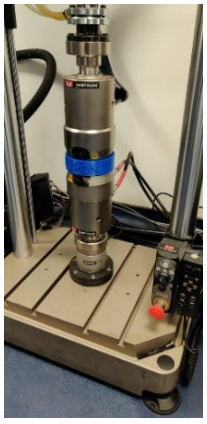

Figure 5: A photograph of the Instron 8874 tensile testing machine used in this study.

Twin disc testing

Due to the Covid-19 outbreak, the intended twin disc test for this project was not conducted, however various documents and input parameters have been verified for a potential future test using the IRR's twin disc rig, seen in Figure 6. Due to these circumstances, it was necessary to compare the tensile data found against the existing wear and RCF data gathered by Burstow and added to by the IRR.

Figure 6: A photograph of the twin disc testing machine at the IRR.

Hardness testing

Hardness testing was not conducted for this project and instead values of hardness for each steel sample were taken from existing IRR hardness data.

RESULTS ANALYSIS

The main purpose of this study is the post-processing and analysis of existing and new damage function data, as well as material property data.

Tensile results

From the tensile tests conducted at the IRR, the data was post-processed to give a stress-strain graph for each rail steel specimen. These graphs were used to find the various material properties stated in the methodology.

Ultimate tensile strength vs hardness

Comparing ultimate tensile strength and hardness shows a strong linear correlation coefficient of 0.91 between the two parameters, as can be seen in Figure 7.

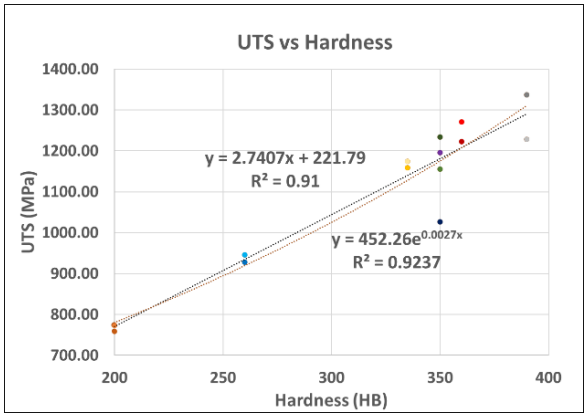

Figure 7: A graph of UTS vs hardness.

Yield strength vs hardness

It was then tested to see if a linear correlation existed between yield strength and hardness, as shown in Figure 8. The data found only shows a 0.63 correlation coefficient, which suggests that hardness tests may not be a good measure of yield strength.

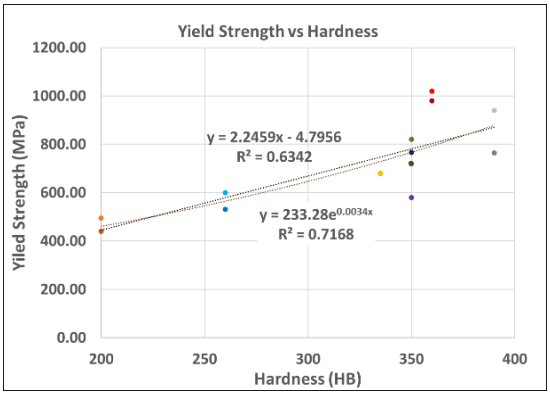

Figure 8: A graph of yield strength vs hardness.

Rail head vs rail foot

The last conclusion to be drawn from the isolated tensile test was that generally, the young's modulus of a material at the head of a rail and the foot of a rail are similar (<5% percentage difference). The UTS at the head and foot of the different rail materials, however, can be seen to have significant differences of above five percent. The most significant discrepancy in material properties at the head and foot of the rail is apparent when analysing the yield strength of the various samples, with most being well over ten percent different (max 24% different). This can be seen in Figure 9. These discrepancies will be discussed further in this project.

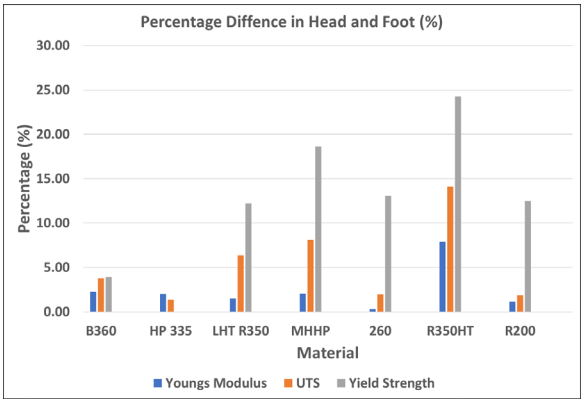

Figure 9: A bar chart of the percentage differences between material properties at the head and foot of a rail.

Wear results

Using existing twin disc data gathered by Burstow and added to by the IRR, as well as the tensile data from the test conducted in this article, significant conclusions were drawn on the link between material properties and wear.

Hardness

The logical first step to improving upon the existing understanding of the effects of material properties on wear was to plot wear rate vs hardness. This is because in many existing wear models, such as Archard's, hardness is the only material property used in the wear rates formulation.

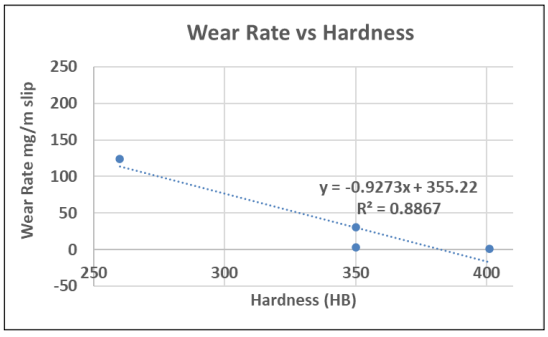

Figure 10: A graph of wear rate vs hardness.

The correlation found in Figure 10, between wear rate and hardness, was found to be strong, negative, and linear ($R^2 = 0.89$), however it was believed this could be improved upon.

Hardness/ young's modulus

To test whether the previously mentioned theory of a ratio of hardness (H) to young's modulus (E) is viable, graphs were plotted of H/E, H/E^2 and H^3/E^2 using the tensile data found, and Burstow's data.

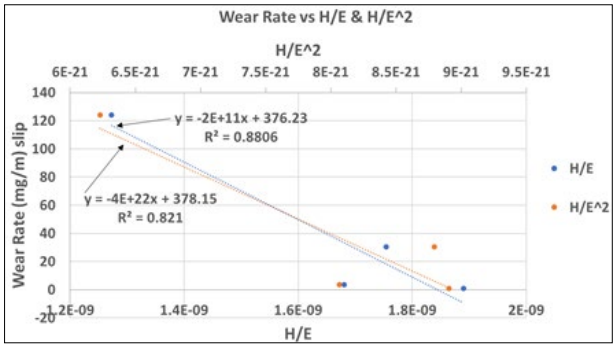

Figure 11: A graph of wear rate vs H/E & H/E^2.

Figure 11 shows that neither the ratio of H/E (R^2= 0.88) or H/E^2 (R^2= 0.82) has a better correlation to wear data than hardness (R^2= 0.89). H/E is a ratio that characterizes a material's resistance to elastic deformation. A ratio of H/E^2 is expected to correlate better with abrasive and erosive wear as it can indicate a material's resistance to permanent damage (Surzhenhov, 2016), however as shown in Figure 11 this is not the case. For the sake of testing the entire theory, the parameter of H^3/E^2 will be analysed. This parameter allows for the estimation of the dissipation of energy at plastic deformation during load within the materials endurance (Surzhenhov, 2016).

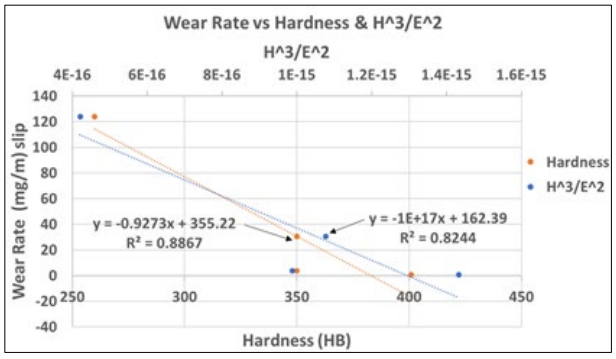

Figure 12: A graph of wear rate vs hardness & H^3/E^2

Figure 12 shows that the ratio of H^3/E^2 (R^2 = 0.82) also shows no greater correlation to wear data than hardness, meaning the addition of the young's modulus may have no impact on the wear, however both Figure 11 and Figure 12 still show a strong linear correlation between the ratio and wear rate, hinting that it could. A high H/E, in the theory mentioned, should be beneficial to wear resistance, which is supported in each of the graphs as they all have strong correlations. Theoretically, a high H/E ratio with a moderately high hardness, has a higher elastic strain to fracture, meaning good toughness properties. However, this could only be true for surfaces with pre-existing flaws or cracks, as generally tougher and more elastic materials (low E) are able to resist abrasive wear well. With flaws present, a stiffer (higher E) material surface could resist the forces that open cracks better (Bhusan, 2001). This could be one of the reasons that the correlation coefficient decreases, as some new evidence suggests that a lower young's modulus value will have more wear resistance than one with similar hardness but higher young's modulus.

Young's modulus/ hardness

After it was observed that the correlation coefficient was reduced in the H/E graphs, the ratio of E/H was plotted, to see if it would have any improvement in the correlation to the wear data. This was expected to increase the correlation more than H/E as Archard's theory includes hardness in the denominator of its formula.

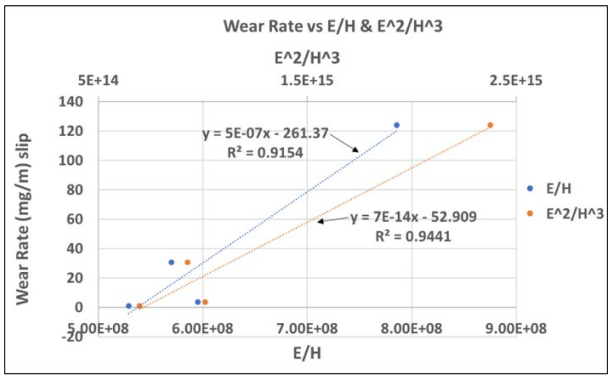

Figure 13: A graph of wear rate vs E/H & E^2/H^3.

Unlike previously, the correlation of the E/H (R^2= 0.92) and E^2/H^3 (R^2= 0.94) ratios to wear rate has improved, as can be seen in Figure 13 as compared to Figure 10. Through a trial-and-error method and an understanding of other material properties, the percentage elongation (Pe) of each material will now be applied to the previous ratio ($(E^2*Pe)/H^3$) to see if it yields better correlation to the wear data.

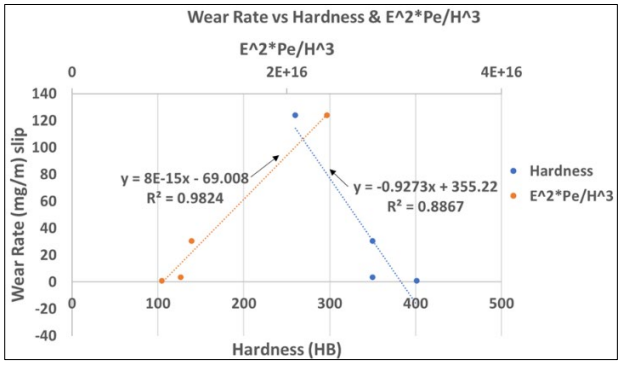

Figure 14: A graph of wear rate vs hardness & E^2*Pe/H^3.

As can be seen in Figure 14, the correlation coefficient of the $(E^2*Pe)/H^3$ ratio to wear data is 0.98, which is much higher than the 0.89 produced by plotting wear versus hardness (Figure 10). This

significant increase in the correlation coefficient may suggest a better model for plotting against wear data and a greater understanding of how more material properties link to wear. This model agrees with Archard's theory, that the inverse of hardness is proportional to wear rate, which partially justifies why the correlation coefficient is better when the hardness is included on the bottom of the ratio in the model discussed in this article.

Figure 14 suggests that a material with a high hardness, a low young's modulus, and low percentage elongation, will have better wear resistive properties. It has been suggested in previous papers that the E/H ratio is a valid parameter to use for estimating the wear rate of materials (Bhusan, 2001). The percentage elongation was included due to a relationship found in a publication on the effects of heat treatment on mechanical properties and the study of the wear behavior of dual-phase steels using air jet erosion testing, written by Sunil Kumar Rajput and other authors. This paper shows a correlation that lower percentage elongation generally means lower wear loss. As percentage elongation is the amount of plastic and elastic deformation a material can take before fracturing, it would make sense to include it on the top of the ratio (E^2/H^3). H^3/E^2 allows the estimation of the dissipation of energy at plastic deformation during loading that a material can endure. With this definition, it is evident as to why the percentage elongation should also be included, as both parameters attempt to measure the plastic deformation to fracture.

Creating a wear rate model

From the near perfect linear relationship shown between $(E^2*Pe)/H^3$ and the wear data from Burstow, led to the derivation of equations to predict wear rate from material properties.

$$\text{Wear Rate}_{\text{New}} = \text{Wear Rate}_{260} - (8E - 15 * (E^2 * Pe)/H^3{}_{260} - (E^2 * Pe)/H^3{}_{\text{New}})$$

(8)

$$\text{Wear Rate}_{\text{New}} = 8E - 15 * \left(\frac{E^2 * Pe}{H^3{}_{\text{New}}}\right) - 69.008$$

(9)

RCF results

The Covid-19 virus unfortunately prevented access to a twin disc rig, meaning no rolling contact fatigue (RCF) data could be gathered. As an alternative to supplement the project, post-processing of RCF data, produced by Burstow, was conducted to help characterize the whole life rail model (WLRM) graph using material properties.

An example of Burstow's characterization of a WLRM graph can be seen in Figure 15, along with Figure 16, which uses data produced by Burstow to show the estimated WLRM function for different rail steels.

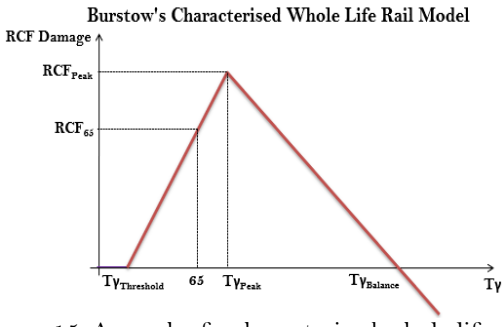

Figure 15: A graph of a characterized whole life rail model of R260 using theories by (Burstow, 2009).

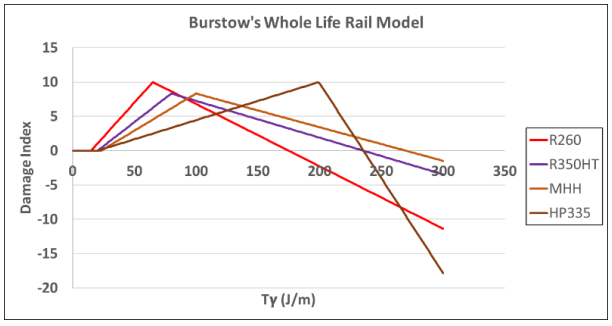

Figure 16: A graph of the various whole life rail estimated model properties of several rail steels, created using data by (Burstow, 2009) and added to by the Institute of Railway Research.

From Figure 15, Burstow derived equations to quantify each of the significant points marked on the graph. These equations are as follows:

$$T\gamma_{\text{Threshold}} = 15 \times \frac{\text{Hardness}_{\text{New Material}}}{\text{Hardness}_{260\ \text{Material}}}$$

(10)

$$T\gamma_{\text{Balance}} = 175 \times \frac{\text{Hardness}_{\text{New Material}}}{\text{Harndess}_{260\ \text{Material}}}$$

(11)

$$RCF_{peak} = 10 \times \frac{Elongation_{260\ Material}}{Elongation_{New\ Material}} \quad (12)$$

$$RCF_{65} = 10 \times \frac{RCF\ Resistance_{260\ Material}}{RCF\ Resistance_{New\ Material}} \quad (13)$$

Hardness vs no. cycles to RCF initiation

Hardness is used to characterise the Tγ Threshold and Tγ Balance in Burstow's WLRM equations, presumably due to its high correlation (0.975) to the number of cycles to initiate RCF cracks, as seen in Figure 17. Tγ Threshold is the Tγ value at which RCF will begin to occur. Tγ Balance is the transition point from RCF to wear. The Tγ Threshold value should be proportional to the number of cycles to RCF initiation, so it is reasonable as to why Burstow uses hardness in his calculation of Tγ Threshold and Tγ Balance.

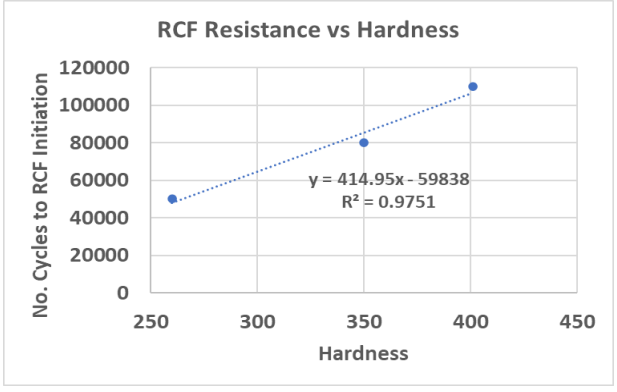

Figure 17: A graph of RCF data plotted against hardness (Burstow,2009).

No. cycles to RCF initiation vs UTS

It was attempted in this study to see if the previously found ratio of $(E^2 * Pe)/H^3$ would yield greater correlation to the RCF resistance of the different steel samples, however this showed a lower correlation than plotting against hardness. Despite this it was found in this study that the average ultimate tensile strength taken from the head and foot of the rail samples, had a perfect correlation ($R^2 = 1$) to the RCF resistance data, used in Burstow's studies. This can be seen in Figure 18.

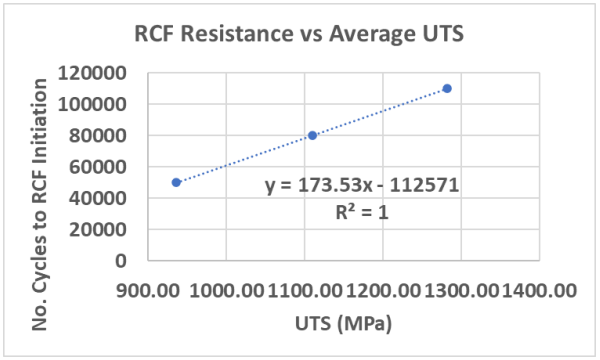

Figure 18: A graph of RCF data plotted against UTS (Burstow, 2009).

UTS whole life rail model

Figure 18 displayed the potential for estimating the initiation of RCF cracks using UTS. Due to this, the Tγ Threshold and Tγ Balance was formulated using UTS data and the existing R260 grade data, to help create a new WLRM graph. This gave the following equations:

$$T\gamma_{Threshold} = 15 \times \frac{UTS_{New\ Material}}{UTS_{260\ Material}} \quad (14)$$

$$T\gamma_{Balance} = 175 \times \frac{UTS_{New\ Material}}{UTS_{260\ Material}} \quad (15)$$

Using these new equations, as well as equation 12 and equation 13, a new WLRM graph was plotted, as seen in Figure 19.

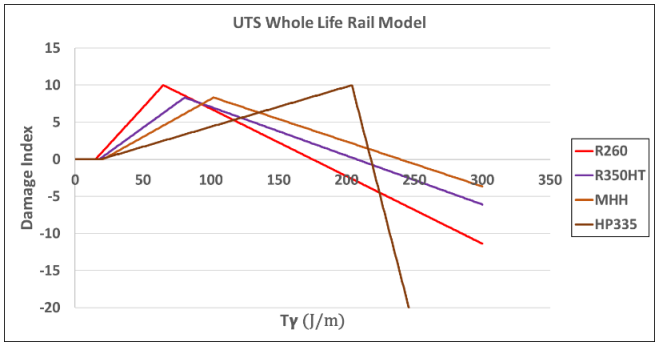

Figure 19: A whole life rail model using UTS equation 13 and equation 14.

When comparing Figure 19 and Figure 16 it can be noted that when using UTS to characterize the WLRM, the Tγ Threshold and Tγ Balance values are lower for all of the steel grades, compared to using hardness, like in Burstow's equations. This implies that each of the steels may begin to experience RCF crack initiation at a lower Tγ than estimated by Burstow's model. As well as this the UTS WLRM estimates that the wear region may begin at a lower Tγ value than estimated by Burstow's WLRM.

Overall, the UTS WLRM shows that the rail steels may have a slightly lower life expectancy than predicted using Burstow's WLRM. Burstow's WLRM and the UTS WLRM do appear very similar due to the high proportionality between hardness and UTS. The rail industry holds the hardness of rail steels to a high regard concerning damage mechanism resistance; however, it may be that the UTS is the important parameter.

DISCUSSION

Detailed analysis of the material properties found in this project could help to support existing findings. For example, the correlation found between hardness and ultimate tensile strength, as seen in Figure 7, may help to support claims that hardness tests can be used as a means of also finding the ultimate tensile strength magnitude, which is a useful finding for saving money when testing rail steels. The material analysis conducted within this project also shows that yield strength is vastly different between the head and foot of a rail, as evidenced in Figure 9. The maximum difference being as high as 24%. This could be investigated in another study to see if this has any effect on the life cycle of a rail and the reasons behind this phenomenon. It is speculated in this study that the heat treatment of samples was the reason for such discrepancies in results. The data showed that HP335, a non-heat-treated specimen, had no difference in yield strength at the head and foot - whilst the other specimens exhibited large differences. The cooling rate of heat-treated samples is said to have a large impact on the yield strength of a material (Ochoa, Williams, & Chawla, 2003).

Comparing material properties to wear within this report has yielded evidence for a potential method of predicting wear rate, which includes material properties that have not been considered in previous railway wear models. The understanding that a ratio of young's modulus squared and percentage elongation to hardness cubed ($(E^2*Pe)/H^3$) could have a potentially large impact on the wear resistive properties of a rail steel, is of high value to the rail industry, with regards to maintenance costing and scheduling. The implications of this project could lead to further testing to prove the model's repeatability and accuracy for use in the industry, and could help to update current damage prediction models, like those discussed in the background research section of this project. Due to Covid-19 preventing tests being conducted for this project and a limited amount of data for analysis, it would be imperative to test that the proposed ratio displays the same correlations shown to the data used in this project.

Comparing material properties to rolling contact fatigue (RCF) in this project, as seen in Figure 17 and Figure 18, led to new ideas for characterizing Mark Burstow's whole life rail model (WLRM). Findings in this report showed that a potentially stronger correlation existed between ultimate tensile strength (UTS) and RCF resistance (R^2 = 1.0) than with hardness and RCF resistance (R^2 = 0.975). This led to the idea that Mark Burstow's WLRM material characterization equations may be more accurate when UTS is included instead of hardness, as can be seen in equations 14 and 15 compared to equations 10 and 11. The UTS data was taken by averaging the UTS of samples from the head and foot of the rail. The material properties found in the tensile test conducted for this study and used in this analysis, may not be an exact match to the material properties of the samples used by Burstow to gather his data. It would be interesting to see further research on this as other material properties such as fracture strain, yield strength and a ratio of ($H^3/(E^2*Pe)$), also showed better correlation to the RCF resistance data than hardness. This may show that ductility and toughness properties must be considered to predict RCF crack initiation and wear properties, and not just hardness. Furthermore, the ability of a material to resist fracture may also be an important parameter in determining the RCF resistance of a material. The new wear model discussed in this project also supports this statement.

CONCLUSION

In conclusion, considering the limitations of this project due to COVID-19, it has successfully

compared experimental tensile test data from several rail steel samples to wear and RCF data which was available in literature. From this a new method for predicting wear has been proposed using material properties not previously considered. This research also provides supporting evidence towards existing findings on the relationship between hardness and ultimate tensile strength. Moreover, it highlights the necessity for further understanding as to why differences in yield strength exist in the foot and head of the rail steel specimens of this report. Further to raising research questions, this project has attempted to offer another possible way of characterizing Mark Burstow's whole life rail model, based on findings in this report. These collective finding should all help to contribute towards offering a better understanding of the link between material properties and damage mechanisms of rails, thus helping to improve maintenance scheduling and costing.

ACKNOWLEDGEMENTS

I would like to say a huge thank you to my project supervisor, Dr Phillip Shackleton, for his advice and support throughout this project, during the lockdown and before the Covid-19 outbreak. I would also like to thank everybody at the Institute of Railway Research for their expertise and aid in publishing this article. Recognition must also be given to the University of Huddersfield for providing materials to aid in the construction of this article.

REFERENCES

Akchurin, A. (2017). *Rolling Contact Fatigue.* Retrieved from https://www.tribonet.org/wiki/rolling-contact-fatigue/

ASTM International. (2021). Steel Standards. 100 Barr Harbor Drive, PO Box C700, West Conshohocken, PA, 19428-2959, *USA: ATSM.* Retrieved from https://www.astm.org/Standards/steel-standards.html

Bandula-Heva, T., & Dhanasekar, M. (2011). Determination of Stress-Strain Characteristics of Railhead Steel using Image Analysis. *International Journal of Mathematical, Computational, Physical and Quantum Engineering, 5*(12). Retrieved from https://eprints.qut.edu.au/48279/1/2012000677.pdf

Bevan, A., Jaiswal, J., Smith , A., & Cabral, M. O. (2018). Judicious Selection of Available Rail Steels to Reduce Life Cycle Costs. *Journal of Rail and Rapid Transit*, 29. doi:https://doi.org/10.1177/0954409718802639

Bhusan, B. (2001). *Modern Tribology Handbook (Vol. 1)*. Columbus, Ohio: CRC Press. Retrieved from https://books.google.co.uk/books?id=h6X0NM7ME8IC&pg=PA840&lpg=PA840&dq=E/H+rati

Braghin, F., Lewis, R., Dwyer-Joyce, R., & Bruni, S. (2006). *A mathematical model to predict railway wheel profile evolution due to wear.* (261 ed.).

Britannica, T. E. (N/A). *Britannica.* Retrieved from https://www.britannica.com/science/Youngs-modulus

British Steel. (2020). HP335 Rail for combatting rolling contact fatigue and wear. PO Box 1, Brigg Road, Scunthorpe, North Lincolnshire, DN16 1BP: *British Steel.* Retrieved from https://britishsteel.co.uk/media/323526/british-steel-hp335-datasheet.pdf

Burstow, M. (2009). *Proposed new WLRM damage functions for alternative rail materials.* 3.

Burstow, M. (2012). VTAC calculator: Guidance note for determining Tγ values. *Network Rail, London.* Retrieved from https://cdn.networkrail.co.uk/wp-content/uploads/2016/12/VTAC-calculator-Guidance-note-for-determining-Tgamma-values.pdf

CORROSIONPEDIA. (2018). *Percent Elongation.* Retrieved from https://www.corrosionpedia.com/definition/6342/percent-elongation

D.Raabe. (N/A). *Nanostructure of pearlitic steels.* Retrieved from http://www.dierk-raabe.com/pearlitic-steels/

F, B., R, L., R.S, D.-J., & S, B. (2006). *A mathematical model to predict railway wheel profile evolution due to wear.*

Galas, R., Smejkal, D., Omasta, M., & Hartl, M. (2014). TWIN-DISC EXPERIMENTAL DEVICE FOR STUDY OF ADHESION IN WHEEL-RAIL CONTACT. *Engineering MECHANICS, 21*(5), 329-334. Retrieved from https://www.researchgate.net/publication/317889979_TWIN-DISC_EXPERIMENTAL_DEVICE_FOR_STUDY_OF_ADHESION_IN_WHEEL-RAIL_CONTACT

Hernandez, E. A. (2008). *Wheel and Rail Contact Simulation Using a Twin Disc Tester.* Thesis Submitted for the Degree of Doctor of

Philosophy, The University of Sheffield, Department of Mechanical Engineering.

Hertz, H. (1881/1896). On the contact of elastic solids. *Miscellaneous Papers*.

Hiensch, M., & Burgelman, N. (2018). ROLLING CONTACT FATIGUE: DAMAGE FUNCTION DEVELOPMENT FROM TWO-DISC TEST DATA. *11th INTERNATIONAL CONFERENCE ON CONTACT MECHANICS AND WEAR OF RAIL/WHEEL SYSTEMS (CM2018)*, *430-431*, 383-390. doi:https://doi.org/10.1016/j.wear.2019.05.028

Hiensch, M., & Burgelman, N. (2018). ROLLING CONTACT FATIGUE: DAMAGE FUNCTION DEVELOPMENT FROM TWO-DISC TEST DATA. *11th INTERNATIONAL CONFERENCE ON CONTACT MECHANICS AND WEAR HANICS AND WEAR*, *430-431*, 376-382. doi:https://doi.org/10.1016/j.wear.2019.05.028

Iwnicki, S. (2006). *Handbook of railway vehicle dynamics*. (S. Iwnicki, A. Wickens, A. Orlova, & More Contributors, Eds.) Manchester: CRC Press, Taylor & Francis Group, LLC.

Lewis, R., Christoforou, P., Wang, W. J., Beagles, A., Burstow, M., & Lewis, S. R. (2019). Investigation of the influence of rail hardness on the wear of rail and wheelmaterials under dry conditions (ICRI wear mapping project). *Wear*, 383-392. doi:https://doi.org/10.1016/j.wear.2019.05.030

Lewis, R., Magel, E., Wang, W.-j., Olofsson, U., Lewis, S., Slatter, T., & Beagles, A. (2017, Feb). Towards a Standard Approach for Wear Testing of Wheel and Rail Materials. *Proceedings of the Institution of Mechanical Engineers Part F Journal of Rail and Rapid Transit*, *231*(7), 1-27. doi:10.1177/0954409717700531

Martins, J. M. (2001). Contact Mechanics. *Proceedings of the 3rd Contact Mechanics International Symposium*, (p. 434). Lisbon.

Molyneux-Berry, P., Davis, C., & Bevan, A. (2014). The Influence of Wheel/Rail Contact Conditions on the Microstructure and Hardness of Railway Wheels. (S. Ubertini, Ed.) *Research Article*, *Volume 2014*(Article ID 209752), 16.

Muhamedsalih, Y., Stow, J., & Bevan, A. (2018). Use of railway wheel wear and damage predictions tools to improve maintenance efficiency through the use of Economic Tyre Turning (ETT). *Proceedings of the Institution of Mechanical Engineers Part F Journal of Rail and Rapid Transit*, p. 24.

Ochoa, F., Williams, J., & Chawla, N. (2003). Effects of cooling rate on the microstructure and tensile behavior of a Sn-3.5wt.%Ag solder. *Journal of Electronic Materials*, 1414-1420. doi:https://doi.org/10.1007/s11664-003-0109-z

Peter, S. (2007). The Fundamentals of Piping Design. *Metallic Materials for Piping Components*, *Chapter 3*, 115-136. Retrieved from https://www.sciencedirect.com/science/article/pii/B9781933762043500126

Pombo, J., Ambrosio, J., Pereira, M., & others, a. (2010). *A RAILWAY WHEEL WEAR PREDICTION TOOL BASED. JOURNAL OF THEORETICAL AND APPLIED MECHANICS*, 770.

Quost, X., Ariaudo, C., Dwyer-Joyce, R., Kuka, N., Lewis, R., & Tassini, N. (2010, February). A numerical model of twin disc test arrangement for the evaluation of railway wheel wear prediction methods. *Wear*, *268*(5-6), 32. doi:10.1016/j.wear.2009.11.003

Rail, N. (2012). VTAC calculator: Guidance note for determining Tγ values., *Issue 1*, p. 7. Retrieved from https://www.networkrail.co.uk/wp-content/uploads/2016/12/VTAC-calculator-Guidance-note-for-determining-Tgamma-values.pdf

Shebani, A., & Iwnicki, S. (2016). The Effect of Surface Condition on Wear of a Railway Wheel and Rail. *International Journal of Mechanical and Mechatronics Engineering*, *10*(9), 8.

Surzhenhov, A. (2016). *Is high hardness and high H/E and H3/E2 associated with brittleness in*. Tallinn University of Technology. Retrieved from https://www.researchgate.net/post/Is_high_hardness_and_high_H_E_and_H3_E2_associat

SUSTRAIL. (n.d.). The sustainable freight railway: Designing he freight vehicle – track system for higher delivered tonnage with improved availability at reduced cost. (A. Beagles, Ed.) *SUSTRAIL Concluding Technical Report*, 198. doi:ISBN: 978-2-7461-2401-1

Tomoya, K., Shigeru, F., & Hamanda , N. (2013). *Proposal for an engineering definition of a fatigue crack initiation unit for evaluating the fatigue limit on the basis of crystallographic analysis of pearlitic steel*. Springer

Science+Business Media Dordrecht. doi:10.1007/s10704-013-9895-3

Wang, Q. J., & Chung, Y.-W. (Eds.). (2013). Hertz Theory: Contact of Spherical Surfaces. *Encyclopedia of Tribology*, 109.

Wangyang, N., Cheng, Y.-T., Lukitsch, M., Weiner, A., & Lev, L. (2004). Effects of the ratio of hardness to Young's modulus on the friction and wear behavior of bilayer coatings. *Applied Physics Letters*, *85*(18).

Yates, J. K. (1996). British Steel: Innovation in Rail Steel. *Science in Parliament*. Retrieved from http://www.phase-trans.msm.cam.ac.uk/parliament.html

ZaaZaa, K., & Schwab, A. (2009, Aug - Sep). REVIEW OF JOOST KALKER'S WHEEL-RAIL CONTACT THEORIES AND THEIR IMPLEMENTATION IN MULTIBODY CODES. *Proceedings of the ASME 2009 International Design Engineering Technical Conferences & Computers and Information in Engineering Conference* (p. 13). San Diego: ASME. Retrieved from https://www.researchgate.net/publication/267488535_Review_of_Joost_Kalker's_Wheel-Rail_Contact_Theories_and_Their_Implementation_in_Multibody_Codes